Journal of Sound and Vibration 329 (2010) 2029–2043

Contents lists available at ScienceDirect

Journal of Sound and Vibration

journal homepage: www.elsevier.com/locate/jsvi

Chatter resistance of non-uniform turning bars with attached dynamic absorbers—Analytical approach

J. Saffury *, E. Altus

Faculty of Mechanical Engineering, Technion, Israel Institute of Technology, Haifa 32000, Israel

ARTICLE INFO

Article history:
Received 28 August 2009
Received in revised form
10 November 2009
Accepted 9 December 2009
Handling Editor M.P. Cartmell
Available online 6 January 2010

ABSTRACT

Forced harmonic vibration of a non-uniform elastic beam with attached dynamic vibration absorbers (DVA) is studied. Analytical approximation of the solution is obtained by the functional perturbation method (FPM). The problem has application to cutting tools operations where the resistance of the tool holder against regenerative chatter can be enhanced by optimizing the real part of the frequency response function (FRF). A test case of a beam with step-like heterogeneity and single DVA at the tip shows that the FPM solution is very accurate for up to ~40 percent deviation in both stiffness and mass density. Using the analytical results and Sims approach, optimal DVA tuning is found for each set of beam heterogeneity parameters by solving a set of nonlinear algebraic equations numerically. It is found that the optimum can be further improved by searching for the best step location. The system optimization is then expanded to a general heterogeneous beam with a DVA at its tip. The mass and stiffness distribution is optimized by applying the Lagrange variation method on the FPM solution yielding Fredholm integral equations. The optimized morphology is found to be approximately linear and far from the "intuitive" step-like one (Rivin and Kang, 1992) and yields better chatter-resistance.

1. Introduction

The subject of free and forced vibration of uniform beams carrying single and multiple one-dof spring-mass-dampers has been studied extensively in the literature. Analytical solutions were obtained by Snowdon [1], Bergman and Nicholson [2–3], Ozguven and Candir [4], Manikanahally and Crocker [5], Gúrgóze [6]. Wu et al. [7–8] combined numerical methods. Although [5] covers non-uniform beams, the natural frequencies are found numerically. Korenev and Reznikov [9] obtained analytically accurate solutions for forced harmonic vibrations of a heterogeneous cantilever beam with an attached single one-dof spring-mass-damper; however, the solutions are limited to specific laws of stiffness and mass variation. Wu [10] investigated the free vibration of a non-uniform cantilever beam carrying multiple two-dof spring-mass-dampers by the finite element method.

In the present paper the solution of forced harmonic vibrations of a non-uniform cantilever beam with multiple spring-mass-dampers is obtained analytically by the functional perturbation method (FPM) (Altus et al. [11,12]). The method can be applied to optimal design of machine tool structures where the cutting tool holder is non-uniform and has large overhang ratio (internal turning tools). The dynamic vibration absorber (DVA) is a passive device with a

* Corresponding author. Tel.: +972 546800283; fax: +972 777808703.
E-mail address: saffury@tx.technion.ac.il (J. Saffury).

0022-460X/$ - see front matter
doi:10.1016/j.jsv.2009.12.015

Nomenclature

b	chip width
c	DVA normalized modal damping
$G_{x\zeta}$	Green's function as a function of x and ζ
k	DVA normalized modal stiffness
K	beam stiffness per unit length
m	DVA normalized mass
M	beam mass per unit length
s	step location
u_1	orientation coefficient
u_{xt}	beam transverse displacement at x location and time t
U_x	beam transverse displacement in the frequency domain
y	displacement of the cutting tool normal to the cutting surface
β	correlation coefficient between stiffness and mass deviations of a beam
ε	relative phase angle of vibration between successive tooth passes
κ	"variation" measure of distributed stiffness of a heterogeneous beam
μ	"variation" measure of distributed mass of a heterogeneous beam
ψ	frequency parameter.
ω	vibration angular frequency

spring-mass-damper model attached to the tool holder (cantilever beam) to attenuate excessive vibrations during the cutting process (Donies and Van Den Noortgate [13]).

Self-excited vibration, known as chatter, causes increased tool wear, and results in a reduction of material removal rate. Understanding and controlling chatter yield reduced costs and higher productivity. Chatter was thought as a result of a negative damping effect [14]. Guerney and Tobias [15] and Tlusty [16] showed that chatter occurs due to regenerative effect and mode coupling. These latter propositions were based on the linear theory of chatter but were able to explain many behavioral patterns of chatter and have led to the development of many control methods. Stability diagrams were derived in the process parameters space. The linear theory, however, fails to explain some patterns like finiteness of chatter amplitude and bifurcations. These phenomena are explained by assuming nonlinearity in the machine tool stiffness, cutting force, and friction induced at the tool-chip interface (Hanna and Tobias [17], Deshpande and Fofana [18], Moon [19], Wiercigroch and Krivtsov [32], Warminski et al. [33], Nosyreva and Molinari [34]). We focus here on the holder heterogeneity effects which are nonlinear, staying with the linear regenerative chatter, and leave the coupling with other nonlinearities, such as discontinuity of the friction characteristics (Wiercigroch and Krivtsov [32]) and nonlinear regenerative effect (Stépán [35]) to future study. The simplified linear theory of chatter is proven not to substantially alter the most important effects on the stability limit as they are found experimentally (Tlusty [20], Moon [19], Moradi et al. [21]).

The DVA device, when tuned properly, can reduce the peak magnitude of the frequency response function (FRF) of the tool holder. This is achieved by using Ormondroyd and Den Hartog's classical 'equal peaks' method (Den Hartog [22]). For improving the chatter stability, other methods have been proposed: analytical (Rivin and Kang [23], Sims [24]), numerical (Liu and Rouch [25], Moradi et al. [21]), and by manual tuning (Tarng et al. [26]).

Rivin and Kang [23] and Sims [24], considered the cantilever tool as a lumped, linear and one dof model. The DVA is considered as an additional linear dof. Saffury and Altus [27] generalized Sims method analytically to the case of continuous uniform beam.

Analytical solutions of stability limit in turning show that the depth of cut dominates the chatter instability, and is inversely proportional to the most negative real value of the FRF (Tlusty [20]).

The "combination structure" proposed by Rivin and Lapin [28] for tool holders is a heterogeneous bar composed of two parts: a root segment (with high Young's modulus), and an overhanging free segment (made of light material). Rivin and Kang [23] optimized the parameters of the combined lumped model with a DVA using the $K\delta$ optimization criteria, where K is the effective stiffness and δ represents the log-decrement damping parameter. Sims [24] optimized separately the magnitude and the real part of the FRF for the lumped mass model. Although Rivin's method offers superior performance over Den Hartog's method, it does not optimize the real part of the FRF [24].

The manuscript is organized as follows. In chapter 2, the FRF of a heterogeneous beam with attached DVAs is solved analytically by the FPM and then examined in chapter 3 by considering a piecewise homogeneous beam for which an exact solution can be derived. In chapter 4, the problem is applied to a cutting tool holder with step-like heterogeneity and single DVA at its tip. The chatter-resistance for a given step heterogeneity is obtained and optimized by tuning the DVA parameters according to Sims approach ([24,27]). In chapter 5 we search for a step location which produces the best optimum. In chapter 6, the optimization is expanded to finding the mass and stiffness distribution of a general heterogeneous beam with single DVA at the tip.

2. Forced vibration of a heterogeneous beam with attached DVAs

In the following, the solution of the forced harmonic vibration of a heterogeneous beam with attached DVAs will be approximated analytically by the FPM. The dynamic governing equation of a non-uniform cantilever beam with a mass M_x

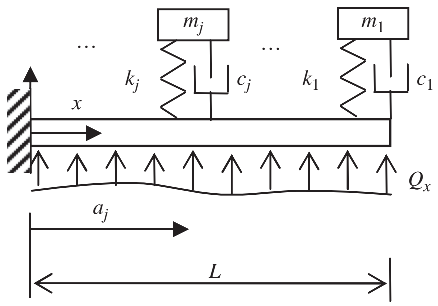

Fig. 1. Cantilever beam with attached spring-mass-damper systems and distributed load.

and (bending) stiffness K_x per unit length, loaded by a distributed load q_{xt} is,

$$(K_x u_{xt,xx})_{,xx} + M_x u_{xt,tt} = q_{xt}; \quad 0 < x < L, \quad t > 0 \tag{1}$$

The Boundary Conditions (BCs) are:

$$u_{xt}|_{x=0} = u_{xt,x}|_{x=0} = K_x u_{xt,xx}|_{x=L} = (K_x u_{xt,xx})_{,x}|_{x=L} = 0; \qquad t > 0 \tag{2}$$

where u_{xt} is the transverse displacement along the beam and it is a function of space (x) and time (t). For a simple harmonic external loading with angular frequency ω:

$$q_{xt} = Q_x e^{\mathrm{i}\omega t}, \tag{3}$$

the forced vibration problem has the steady-state solution:

$$u_{xt} = U_x e^{\mathrm{i}\omega t}. \tag{4}$$

The system includes n attached DVAs having springs k_j, viscous dampers c_j and masses m_j, located at a_j (Fig. 1). The displacement amplitude of a DVA mass (m_j) in the frequency domain is,

$$w_j = H_j U_{a_j} \ (no\ summation), \quad H_j = \left(1 - \frac{m_j \omega^2}{k_j + c_j \mathrm{i}\omega}\right)^{-1}, \tag{5}$$

where H_j is the amplification between w_j and the cantilever transverse displacement at a_j.

Substituting (3) and (4) into (1), and taking into account the inertial forces of the DVAs, the governing equation in the frequency domain is therefore:

$$J \equiv (K_x U_{x,xx})_{,xx} - \omega^2 M_x U_x - Q_x - \sum_{j=1}^{n} m_j \omega^2 H_j U_x \delta_{xa_j} = 0; \quad 0 < x < L, \tag{6}$$

with BCs:

$$U_x|_{x=0} = 0, \quad U_{x,x}|_{x=0}, \quad (K_x U_{x,xx})|_{x=L} = 0, \quad (K_x U_{x,xx,x})|_{x=L} = 0, \tag{7}$$

where J is defined in (6) for convenience. Equation (6) is true for any given stiffness and mass morphology; therefore, by the FPM ([11,12]), J and its functional derivatives with respect to these morphologies, near homogeneous fields ($M^{(0)}$, $K^{(0)}$), have to vanish too, i.e.,

$$J_{,K_{x_1} \cdots K_{x_i} M_{\xi_1} \cdots M_{\xi_j}}|_{\substack{K_x = K^{(0)} \\ M_\xi = M^{(0)}}} = 0. \tag{8}$$

This yields a set of PDEs for each order of differentiation. The zero-order equation is:

$$K^{(0)} U^{(0)}_{x,xxxx} - M^{(0)} \omega^2 U^{(0)}_x = Q_x + \sum_{j=1}^{n} m_j \omega^2 H_j U^{(0)}_x \delta_{xa_j}$$

$$\text{BCs}: \quad U^{(0)}_x|_{x=0} = U^{(0)}_{x,x}|_{x=0} = U^{(0)}_{x,xx}|_{x=L} = U^{(0)}_{x,xxx}|_{x=L} = 0, \tag{9}$$

where $U^{(0)}$ is the transverse displacement of the corresponding homogeneous beam, i.e. for M_x=$M^{(0)}$ and K_x=$K^{(0)}$. The first-order equations, which are obtained by functionally differentiating J by "K_{x_1}" and "M_{x_1}", respectively, are:

$$K^{(0)} U^{(K)}_{xx_1,xxxx} - M^{(0)} \omega^2 U^{(K)}_{xx_1} = -(\delta_{xx_1} U^{(0)}_{x,xx})_{,xx} + \sum_{j=1}^{n} m_j \omega^2 H_j U^{(K)}_{xx_1} \delta_{xa_j}$$

$$\text{BCs}: \quad U^{(K)}_{xx_1}|_{x=0} = U^{(K)}_{xx_1,x}|_{x=0} = U^{(K)}_{xx_1,xx}|_{x=L} = U^{(K)}_{xx_1,xxx}|_{x=L} = 0, \tag{10}$$

and,

$$K^{(0)}U^{(M)}_{xx_1,xxxx}-M^{(0)}\omega^2 U^{(M)}_{xx_1}=\omega^2\delta_{xx_1}U^{(0)}_x+\sum_{j=1}^{n}m_j\omega^2 H_j U^{(M)}_{xx_1}\delta_{xa_j}$$
$$\text{BCs}:\quad U^{(M)}_{xx_1}|_{x=0}=U^{(M)}_{xx_1,x}|_{x=0}=U^{(M)}_{xx_1,xx}|_{x=L}=U^{(M)}_{xx_1,xxx}|_{x=L}=0, \tag{11}$$

where,

$$U^{(M)}_{xx_1}\equiv U_{x,M_{x_1}}|_{\substack{M_x=M^{(0)}\\K_x=K^{(0)}}};\quad U^{(K)}_{xx_1}\equiv U_{x,K_{x_1}}|_{\substack{M_x=M^{(0)}\\K_x=K^{(0)}}}. \tag{12}$$

The second-order equations related to differentiating by "$K_{x_1}K_{x_2}$", "$M_{x_1}M_{x_2}$" and "$K_{x_1}M_{x_2}$", respectively, are:

$$K^{(0)}U^{(K_1K_2)}_{xx_1x_2,xxxx}-M^{(0)}\omega^2 U^{(K_1K_2)}_{xx_1x_2}=-(\delta_{xx_1}U^{(K)}_{xx_2,xx}+\delta_{xx_2}U^{(K)}_{xx_1,xx})_{,xx}+\sum_{j=1}^{n}m_j\omega^2 H_j U^{(K_1K_2)}_{xx_1x_2}\delta_{xa_j}$$
$$\text{BCs}:\quad U^{(K_1K_2)}_{xx_1x_2}|_{x=0}=U^{(K_1K_2)}_{xx_1x_2,x}|_{x=0}=U^{(K_1K_2)}_{xx_1x_2,xx}|_{x=L}=U^{(K_1K_2)}_{xx_1x_2,xxx}|_{x=L}=0, \tag{13}$$

$$K^{(0)}U^{(M_1M_2)}_{xx_1x_2,xxxx}-M^{(0)}\omega^2 U^{(M_1M_2)}_{xx_1x_2}=\omega^2(\delta_{xx_1}U^{(M)}_{xx_2}+\delta_{xx_2}U^{(M)}_{xx_1})+\sum_{j=1}^{n}m_j\omega^2 H_j U^{(M_1M_2)}_{xx_1x_2}\delta_{xa_j} \tag{14}$$
$$\text{BCs}:\quad U^{(M_1M_2)}_{xx_1x_2}|_{x=0}=U^{(M_1M_2)}_{xx_1x_2,x}|_{x=0}=U^{(M_1M_2)}_{xx_1x_2,xx}|_{x=L}=U^{(M_1M_2)}_{xx_1x_2,xxx}|_{x=L}=0,$$

and,

$$K^{(0)}U^{(K_1M_2)}_{xx_1x_2,xxxx}-M^{(0)}\omega^2 U^{(K_1M_2)}_{xx_1x_2}=\omega^2\delta_{xx_2}U^{(K)}_{xx_1}-(\delta_{xx_1}U^{(M)}_{xx_2,xx})_{,xx}+\sum_{j=1}^{n}m_j\omega^2 H_j U^{(K_1M_2)}_{xx_1x_2}\delta_{xa_j} \tag{15}$$
$$\text{BCs}:\quad U^{(K_1M_2)}_{xx_1x_2}|_{x=0}=U^{(K_1M_2)}_{xx_1x_2,x}|_{x=0}=U^{(K_1M_2)}_{xx_1x_2,xx}|_{x=L}=U^{(K_1M_2)}_{xx_1x_2,xxx}|_{x=L}=0,$$

where,

$$U^{(M_1M_2)}_{xx_1x_2}\equiv U_{x,M_{x_1}M_{x_2}}|_{\substack{M_x=M^{(0)}\\K_x=K^{(0)}}};\quad U^{(K_1K_2)}_{xx_1x_2}\equiv U_{x,K_{x_1}K_{x_2}}|_{\substack{M_x=M^{(0)}\\K_x=K^{(0)}}};\quad U^{(K_1M_2)}_{xx_1x_2}\equiv U_{x,K_{x_1}M_{x_2}}|_{\substack{M_x=M^{(0)}\\K_x=K^{(0)}}}. \tag{16}$$

All of the PDE's (9)–(15) are non-homogeneous equations of the form:

$$K^{(0)}\tilde{U}_{x,xxxx}-M^{(0)}\omega^2\tilde{U}_x=\tilde{Q}_x$$
$$\text{BCs}:\ \tilde{U}_x|_{x=0}=\tilde{U}_{x,x}|_{x=0}=\tilde{U}_{x,xx}|_{x=L}=\tilde{U}_{x,xxx}|_{x=L}=0. \tag{17}$$

The solution of this problem can be obtained by using the Green's function method:

$$\tilde{U}_x=G_{x\xi}*\tilde{Q}_\xi. \tag{18}$$

where $G_{x\zeta}$ is the solution of BVP (17) for $\tilde{Q}_x=\delta_{x\xi}$. Thus, the solution of (9) is:

$$U^{(0)}_x=G_{x\xi}*Q_\xi+\sum_{j=1}^{n}\omega^2 m_j H_j U^{(0)}_{a_j}G_{xa_j}. \tag{19}$$

The displacement at x=a_j for the homogeneous case ($U^{(0)}_{a_j}$) is obtained by using the "work method" [9]:

$$U^{(0)}_{a_i}=A^{-1}_{ij}B^{(0)}_j. \tag{20}$$

A_{ij} and $B^{(0)}_j$ are defined by,

$$A_{ij}=\delta_{ij}-\omega^2 m_j H_j G_{a_ia_j}\ (\textit{no summation});\quad B^{(0)}_j=G_{a_j\xi}*Q_\xi, \tag{21}$$

where δ_{ij} is Kronecker delta. The solution of (10) and (11), respectively, are:

$$U^{(K)}_{xx_1}=-G_{xx_1,x_1x_1}U^{(0)}_{x_1,x_1x_1}+\sum_{j=1}^{n}m_j\omega^2 H_j U^{(K)}_{a_jx_1}G_{xa_j}, \tag{22}$$

$$U^{(M)}_{xx_1}=\omega^2 G_{xx_1}U^{(0)}_{x_1}+\sum_{j=1}^{n}m_j\omega^2 H_j U^{(M)}_{a_jx_1}G_{xa_j}, \tag{23}$$

where

$$U^{(K)}_{a_ix_1}=A^{-1}_{ij}B^{(K)}_j;\quad B^{(K)}_j=-G_{a_jx_1,x_1x_1}U^{(0)}_{x_1,x_1x_1}, \tag{24}$$

and

$$U^{(M)}_{a_ix_1}=A^{-1}_{ij}B^{(M)}_j;\quad B^{(M)}_j=\omega^2 U^{(0)}_{x_1}G_{a_jx_1}. \tag{25}$$

The solution of (13)–(15), respectively, are:

$$U^{(K_1K_2)}_{xx_1x_2} = -G_{xx_1,x_1x_1}U^{(K)}_{x_1x_2,x_1x_1} - G_{xx_2,x_2x_2}U^{(K)}_{x_2x_1,x_2x_2} + \sum_{j=1}^{n} m_j\omega^2 H_j U^{(K_1K_2)}_{a_jx_1x_2}G_{xa_j}, \tag{26}$$

$$U^{(M_1M_2)}_{xx_1x_2} = \omega^2(G_{xx_1}U^{(M)}_{x_1x_2} + G_{xx_2}U^{(M)}_{x_2x_1}) + \sum_{j=1}^{n} m_j\omega^2 H_j U^{(M_1M_2)}_{a_jx_1x_2}G_{xa_j}, \tag{27}$$

$$U^{(K_1M_2)}_{xx_1x_2} = \omega^2 G_{xx_2}U^{(K)}_{x_2x_1} - G_{xx_1,x_1x_1}U^{(M)}_{x_1x_2,x_1x_1} + \sum_{j=1}^{n} m_j\omega^2 H_j U^{(K_1M_2)}_{a_jx_1x_2}G_{xa_j}, \tag{28}$$

where

$$U^{(K_1K_2)}_{a_ix_1x_2} = A^{-1}_{ij}B^{(K_1K_2)}_j; \quad B^{(K_1K_2)}_j = -(G_{a_jx_1,x_1x_1}U^{(K)}_{x_1x_2,x_1x_1} + G_{a_jx_2,x_2x_2}U^{(K)}_{x_2x_1,x_2x_2}), \tag{29}$$

$$U^{(M_1M_2)}_{a_ix_1x_2} = A^{-1}_{ij}B^{(M_1M_2)}_j; \quad B^{(M_1M_2)}_j = \omega^2(G_{a_jx_1}U^{(M)}_{x_1x_2} + G_{a_jx_2}U^{(M)}_{x_2x_1}). \tag{30}$$

and

$$U^{(K_1M_2)}_{a_ix_1x_2} = A^{-1}_{ij}B^{(K_1M_2)}_j; \quad B^{(K_1M_2)}_j = \omega^2 G_{a_jx_2}U^{(K)}_{x_2x_1} - G_{a_jx_1,x_1x_1}U^{(M)}_{x_1x_2,x_1x_1}. \tag{31}$$

Therefore, the solution for forced harmonic vibrations of the heterogeneous beam with attached DVAs is approximated by Fréchet functional series:

$$U_x = U^{(0)}_x + U^{(K)}_{xx_1} * K'_{x_1} + U^{(M)}_{xx_1} * M'_{x_1} + \tfrac{1}{2}(U^{(K_1K_2)}_{xx_1x_2} ** K'_{x_1}\,K'_{x_2} + U^{(M_1M_2)}_{xx_1x_2} ** M'_{x_1}\,M'_{x_2} + 2U^{(K_1M_2)}_{xx_1x_2} ** K'_{x_1}\,M'_{x_2}) + \cdots. \tag{32}$$

3. A heterogeneous turning bar with a single DVA

The aim of this chapter is to validate and examine the general FPM solution outlined in chapter 2 by considering a heterogeneous-piecewise homogeneous cantilever beam for which an exact solution can be derived. For simplicity single DVA and concentrated loading at the beam tip are analyzed.

The zero-order and first-order coefficients are:

$$\begin{aligned} U^{(0)}_x &= \phi G_{xL} \\ U^{(K)}_{xx_1} &= -g_{Lx_1,x_1x_1}g_{xx_1,x_1x_1} \\ U^{(M)}_{xx_1} &= \omega^2 g_{Lx_1}g_{xx_1}. \end{aligned} \tag{33}$$

The coefficients for the second order are:

$$\begin{aligned} U^{(K_1K_2)}_{xx_1x_2} &= -g_{xx_1,x_1x_1}U^{(K)}_{x_1x_2,x_1x_1} - g_{xx_2,x_2x_2}U^{(K)}_{x_2x_1,x_2x_2} \\ U^{(M_1M_2)}_{xx_1x_2} &= g_{xx_1}U^{(M)}_{x_1x_2}\omega^2 + g_{xx_2}U^{(M)}_{x_2x_1}\omega^2 \\ U^{(K_1M_2)}_{xx_1x_2} &= g_{xx_2}U^{(K)}_{x_2x_1}\omega^2 - g_{xx_1,x_1x_1}U^{(M)}_{x_1x_2,x_1x_1}. \end{aligned} \tag{34}$$

$g_{x\xi}$ and ϕ are defined by:

$$g_{x\xi} = G_{x\xi} + m\omega^2 H\phi G_{xL}G_{L\xi}; \quad \phi \equiv (1-\omega^2 mHG_{LL})^{-1}. \tag{35}$$

Inserting (33) and (34) into (32) yields:

$$\begin{aligned} U_x = {} & \phi G_{xL} - \phi G_{Lx_1,x_1x_1}g_{xx_1,x_1x_1} * K'_{x_1} + \omega^2\phi G_{Lx_1}g_{xx_1} * M'_{x_1} + \phi G_{Lx_2,x_2x_2}g_{xx_1,x_1x_1}g_{x_1x_2,x_1x_1x_2x_2} ** K'_{x_1}\,K'_{x_2} + \omega^4\phi G_{Lx_2}g_{xx_1}g_{x_1x_2} \\ & ** M'_{x_1}\,M'_{x_2} - 2\phi\omega^2 G_{Lx_1,x_1x_1}g_{xx_2}g_{x_2x_1,x_1x_1} ** K'_{x_1}\,M'_{x_2}. \end{aligned} \tag{36}$$

A dimensionless frequency parameter ψ is defined by,

$$\psi^4 = \frac{\omega^2 L^4 M^{(0)}}{K^{(0)}}. \tag{37}$$

Using non-dimensional parameters without re-notations:

$$\begin{aligned} &\frac{x}{L} \to x; \quad \frac{\xi}{L} \to \xi; \quad \frac{x_1}{L} \to x_1; \quad \frac{x_2}{L} \to x_2 \\ &\frac{K_{x_1}}{K^{(0)}} \to K_{x_1}; \quad \frac{M_{x_1}}{M^{(0)}} \to M_{x_1}; \quad \frac{K^{(0)}G_{x\xi}}{L^3} \to G_{x\xi}; \quad \frac{K^{(0)}U_x}{L^3} \to U_x \\ &\frac{K^{(0)}U^{(0)}_x}{L^3} \to U^{(0)}_x; \quad \frac{m}{M^{(0)}L} \to m; \quad \frac{k}{K^{(0)}/L^3} \to k; \quad \frac{c}{\sqrt{K^{(0)}M^{(0)}/L^2}} \to c. \end{aligned} \tag{38}$$

The dimensionless response at the tip of the cantilever (FRF) is therefore:

$$U_1 = g_{11} + \psi^4 g_{1x_1}^2 * M'_{x_1} - g_{1x_1,x_1x_1}^2 * K'_{x_1} + g_{1x_2,x_2x_2} g_{1x_1,x_1x_1} g_{x_1x_2,x_1x_1x_2x_2} ** K'_{x_1} K'_{x_2} + \psi^8 g_{1x_1} g_{1x_2} g_{x_1x_2}$$
$$** M'_{x_1} M'_{x_2} - 2\psi^4 g_{1x_2} g_{1x_1,x_1x_1} g_{x_1x_2,x_1x_1} ** K'_{x_1} M'_{x_2}, \tag{39}$$

where

$$g_{x\xi} = G_{x\xi} + m\psi^4 H\phi G_{x1} G_{1\xi}; \quad H = \left(1 - \frac{m\psi^4}{k + \psi^2 ci}\right)^{-1}; \quad \phi = (1 - m\psi^4 H G_{11})^{-1}. \tag{40}$$

The real part of the FRF (denoted in the following by R) is therefore (39):

$$R \equiv \mathrm{Re}[U_1] = f^{(0)} + f_{x_1}^{(1)} * M'_{x_1} + f_{x_1}^{(2)} * K'_{x_1} + f_{x_1x_2}^{(3)} ** M'_{x_1} M'_{x_2} + f_{x_1x_2}^{(4)} ** K'_{x_1} K'_{x_2} + f_{x_1x_2}^{(5)} ** K'_{x_1} M'_{x_2}, \tag{41}$$

where,

$$f^{(0)} = \mathrm{Re}[\phi] G_{11}; \quad f_{x_1}^{(1)} = \mathrm{Re}[\phi^2] \cdot \psi^4 G_{1x_1}^2; \quad f_{x_1}^{(2)} = -\mathrm{Re}[\phi^2] \cdot G_{1x_1,x_1x_1}^2;$$
$$f_{x_1x_2}^{(3)} = \psi^8 G_{1x_1} G_{1x_2} (\mathrm{Re}[\phi^2] G_{x_1x_2} + \mathrm{Re}[\alpha\phi^2] G_{x_1 1} G_{1x_2});$$
$$f_{x_1x_2}^{(4)} = (G_{1x_1} G_{\psi x_2})_{,x_1x_1x_2x_2} (\mathrm{Re}[\phi^2] G_{x_1x_2} + \mathrm{Re}[\alpha\phi^2] G_{1x_1} G_{1x_2})_{,x_1x_1x_2x_2};$$
$$f_{x_1x_2}^{(5)} = -2\psi^4 (G_{1x_1} G_{1x_2})_{,x_1x_1} (\mathrm{Re}[\phi^2] G_{x_1x_2} + \mathrm{Re}[\alpha\phi^2] G_{x_1 1} G_{1x_2})_{,x_1x_1}. \tag{42}$$

α is defined by

$$\alpha = m\psi^4 H\phi. \tag{43}$$

The corresponding Green's function of the BVP (17) is obtained analytically using Krylov's functions [9]:

$$G_{x\xi} = \begin{cases} \frac{1}{2}(\cos(x\psi) - \cosh(x\psi)) B_\xi + \frac{1}{2}(\sin(x\psi) - \sinh(x\psi)) D_\xi & 0 < x < \xi < 1 \\ \frac{1}{2}(\cos(\xi\psi) - \cosh(\xi\psi)) B_x + \frac{1}{2}(\sin(\xi\psi) - \sinh(\xi\psi)) D_x & 0 < \xi < x < 1 \end{cases}. \tag{44}$$

B_ξ and D_ξ are initial parameters (moment and shear force at x=0):

$$B_\xi = \frac{-d_2 \sin(\xi\psi) - d_1 \sinh(\xi\psi) + d_3(\cos(\xi\psi) - \cosh(\xi\psi))}{2\psi^3(1 + \cos(\psi)\cosh(\psi))}, \tag{45}$$

$$D_\xi = \frac{d_1 \cos(\xi\psi) + d_2 \cosh(\xi\psi) + d_4(\sin(\xi\psi) - \sinh(\xi\psi))}{2\psi^3(1 + \cos(\psi)\cosh(\psi))}, \tag{46}$$

where,

$$d_1 = 1 + \cos(\psi)\cosh(\psi) - \sin(\psi)\sinh(\psi); \quad d_2 = 1 + \cos(\psi)\cosh(\psi) + \sin(\psi)\sinh(\psi)$$
$$d_3 = \sin(\psi)\cosh(\psi) - \cos(\psi)\sinh(\psi); \quad d_4 = \sin(\psi)\cosh(\psi) + \cos(\psi)\sinh(\psi). \tag{47}$$

For illustration and comparison with exact solutions, we examine the case of a combined step-like morphology of stiffness and mass (Fig. 2):

$$M'_x = \begin{cases} \Delta_M & x < s \\ -\Delta_M & x > s \end{cases}; \quad K'_x = \begin{cases} \Delta_K & x < s \\ -\Delta_K & x > s \end{cases}; \quad 0 < s < 1. \tag{48}$$

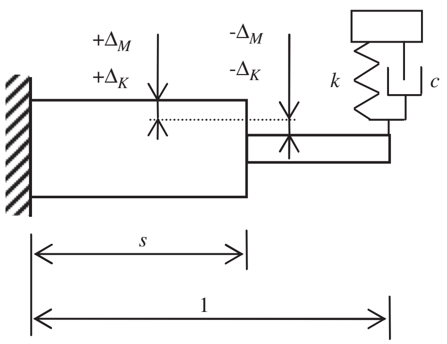

Fig. 2. A cantilever beam with a step-like morphology and attached DVA at the tip.

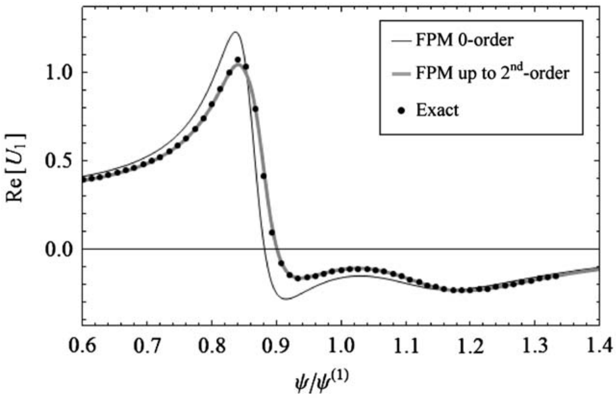

Fig. 3. Re[U_1] of the heterogeneous beam, for the DVA parameters: m=0.1, c=0.2, k=1.1, and morphology: s=0.5, Δ_K=Δ_M=0.05.

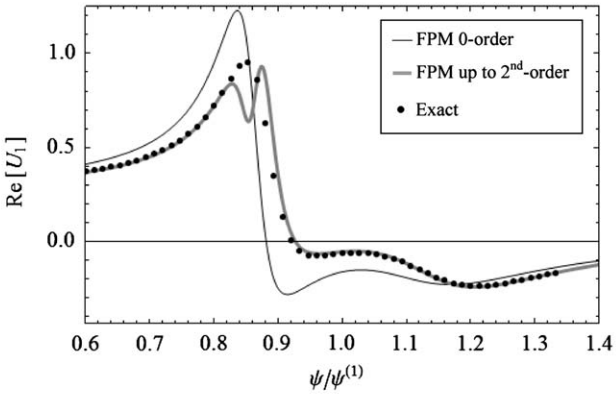

Fig. 4. Re[U_1] of the heterogeneous beam, for the DVA parameters: m=0.1, c=0.2, k=1.1, and morphology: s=0.5, Δ_K=Δ_M=0.1.

The integrals in (41) are obtained by using *Mathematica* software. Re[U_1] is shown in Fig. 3 for the DVA parameters: m=0.1, k=1.1 and c=0.2, and for (normalized) mass and stiffness deviation of Δ_K=Δ_M=0.05. A comparison with exact solution based on two homogeneous regions shows that the zero order term in the FPM series is not sufficient and far from the exact one. However, the second-order approximation is very accurate. Fig. 4 shows the same comparison for greater deviations Δ_K=Δ_M=0.1. The FPM second-order approximation is very accurate for most of the frequency range. A local region around the maximum point reveals a small diversion. Nevertheless, for optimization purposes which will be discussed in the following, the low accuracy region is not involved.

4. Chatter resistance optimization for heterogeneous turning bar with DVA

In the present chapter the condition for the stability of turning bars against regenerative chatter will be first introduced according to [29]. Then the chatter-resistance of a heterogeneous tool holder will be optimized by tuning the DVA parameters correctly.

Tlusty and Polacek [29] introduced the condition for regenerative chatter in turning operation considering the orthogonal cutting case. The system of workpiece and cutting tool are linear and characterized by two individual modes of vibration (directions x_1 and x_2 in Fig. 5). The cutting force f is assumed directly proportional to the chip area, and has a constant direction φ. Vibration amplitudes y_0 and y represent the wavy surfaces before and after a cutting pass, respectively, with a phase shift ε. For simplicity we consider the case where the principal directions of the beams' moments of inertia are orthogonal to the cutting surface. The chip width (b) at the stability limit point is [20]:

$$b_{\lim} = \frac{-1}{2K_s u_1 \,\mathrm{Re}(F_1)}. \tag{49}$$

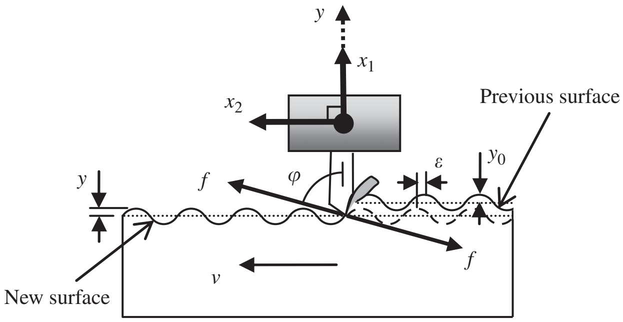

Fig. 5. The regeneration diagram relating force, surface waviness and vibration.

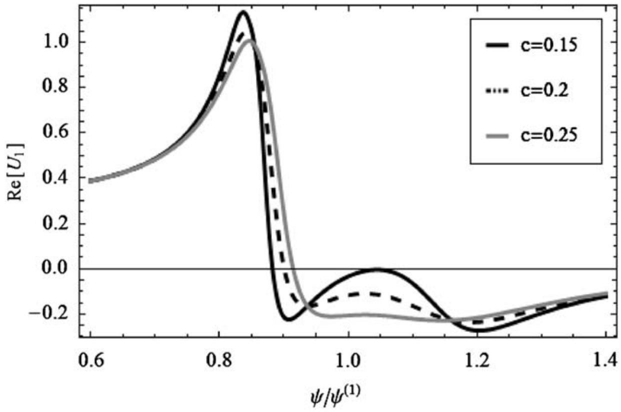

Fig. 6. $\mathrm{Re}[U_1]$ for DVA parameters m=0.1, k=1.1 and three different values of c.

K_s (N/m^2) is a workpiece material constant, F_1 is the transfer function (TF) in direction x_1, and u_1 is an orientation factor ($u_1=\cos(\varphi)$). For positive orientation factor u_1, the smallest chip width at which chatter may occur is:

$$b_{\mathrm{lim,cr}} = \frac{-1}{2K_s u_1 \min[\mathrm{Re}(F_1)]}. \tag{50}$$

where $\min(\mathrm{Re}(F_1))$ denotes the most negative (minimum) real part of F_1. Note that if u_1 is negative, the chatter stability is dictated by the most positive real part of F_1 ($\max[\mathrm{Re}(F_1)]$) which should be decreased for increasing $b_{\mathrm{lim,cr}}$

The cantilever beam analyzed in chapter 3 may represent a heterogeneous tool holder with attached DVA, therefore $F_1=U_1$. A step-like morphology with a single DVA attached to its tip is considered. This specific choice is used as a validation test for the FPM accuracy and also follows the intuitive design by Rivin and Kang [23]. Tuning the DVA parameters for optimal response is done by generalizing Sims approach for a lumped mass model [24,27] to the case of heterogeneous continuous beams.

Fig. 6 describes the response ($\mathrm{Re}[U_1]$) of a cantilever with $\Delta_K=\Delta_M=0.05$ and selected DVA parameters for 3 different c values. Three damping-independent (locked) frequencies, noted as $\psi^{(p)}$, $\psi^{(n)}$ and $\psi^{(a)}$ (after [24]), are identified near $\psi=\psi^{(1)}=1.8751$ which is the first frequency parameter of a fixed-free homogeneous beam. Calculating these points is commonly done by inserting $c\to 0$ and $c\to\infty$ into (41) and looking for ψ which causes $\mathrm{Re}[U_1]$ to be singular [24,27]. However, the FPM is less accurate near these points for an undamped system. We therefore look for locked points by taking another approach which, as far as we know, has not been implemented yet in the literature. Search for ψ which causes the first derivative of the response with respect to c to vanish:

$$\left.\frac{\partial\,\mathrm{Re}[U_1]}{\partial c}\right|_{\psi\,=\,\psi^{(a)},\psi^{(n)},\psi^{(p)}} = 0. \tag{51}$$

This condition is "local", i.e. reflects ψ values for which $\mathrm{Re}[U_1]$ is locally invariant with respect to c. In order to estimate the extent of this "range of invariance" the solution of (51) is shown in Fig. 7, i.e. ψ as a function of c. It is seen that $\psi^{(n)}$, $\psi^{(n)}$ and $\psi^{(p)}$ are practically constant except at very small c. Going back to the explicit expression of (51) it can be shown that it is essentially a third-order polynomial in c, in which the linear part dominates the solution. Therefore, (51) practically leads

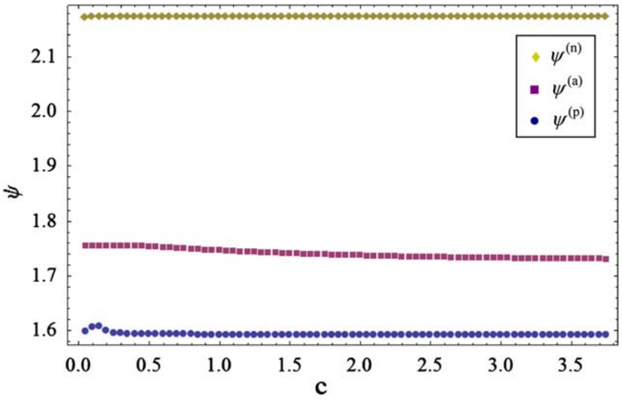

Fig. 7. Local locked-frequencies for DVA parameters m=0.1, k=1.1 and s=0.5, $\Delta_K=\Delta_M$=0.05.

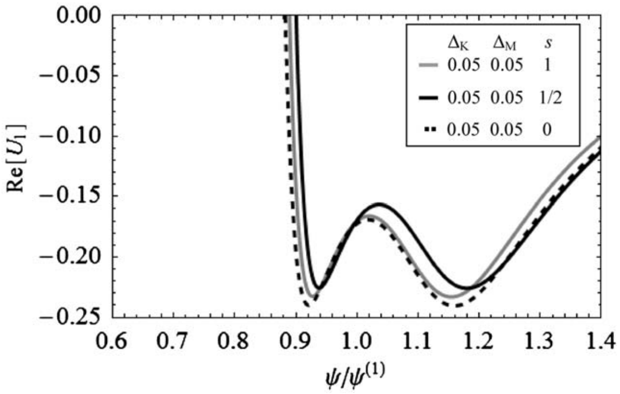

Fig. 8. Comparison Re[U_1] at optimally tuned DVA between homogeneous and heterogeneous beams.

to "global" locked points for a wide range of c. It can be shown that for a lumped mass model (51) is identical to the common $c\to 0$ and $c\to\infty$ method.

For optimal tuning, Re[U_1] at the locked points $\psi^{(a)}$ and $\psi^{(n)}$ has to be equal and also located at local minima. Therefore, the following three conditions have to be fulfilled:

$$\mathrm{Re}[U_1]|_{\psi^{(a)}} = \mathrm{Re}[U_1]|_{\psi^{(n)}}; \quad \frac{\partial\,\mathrm{Re}[U_1]}{\partial\psi}\bigg|_{\psi^{(a)}} = 0; \quad \frac{\partial\,\mathrm{Re}[U_1]}{\partial\psi}\bigg|_{\psi^{(n)}} = 0. \tag{52}$$

However, for a selected value of m we have only two unknowns (c and k) to determine. Sims suggested an approximation based on two of the three sets of equations: (52 a,b) and (52 a,c) and taking the average value from the two partial solutions, i.e.,

$$c = \tfrac{1}{2}(c^{(a)} + c^{(n)}). \tag{53}$$

It is found that for the present heterogeneous case, better response is obtained by non-equal weights:

$$c = \tfrac{2}{3}\,c^{(a)} + \tfrac{1}{3}c^{(n)}. \tag{54}$$

For illustration, Re[U_1] described in Fig. 3 is optimized by tuning the DVA parameters according to the above method. The optimal response is shown in Fig. 8 (s=1/2) around the negative range. The heterogeneous case is also compared to other two homogeneous limit cases: s=1 and s=0. An improvement of 5.5 percent and 8.3 percent in the optimal chatter resistance is achieved by s=1/2 relative to s=1 and s=0, respectively.

5. Further optimization by searching for optimal *s*

In the previous chapter, the optimal chatter resistance for a given s has been investigated. Here we search for s which produces the best optimum.

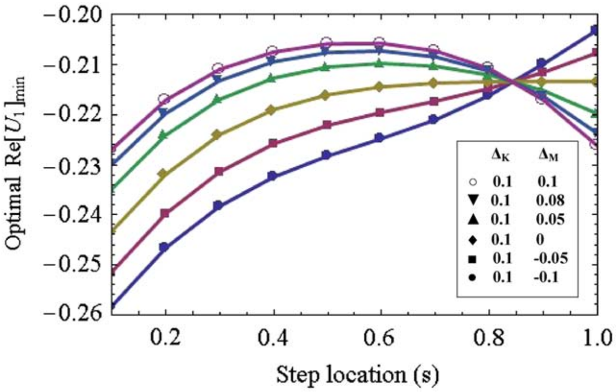

Fig. 9. Re$[U_1]_{\min}$ at optimal tuning of the DVA parameters and for step-like morphology of the beam.

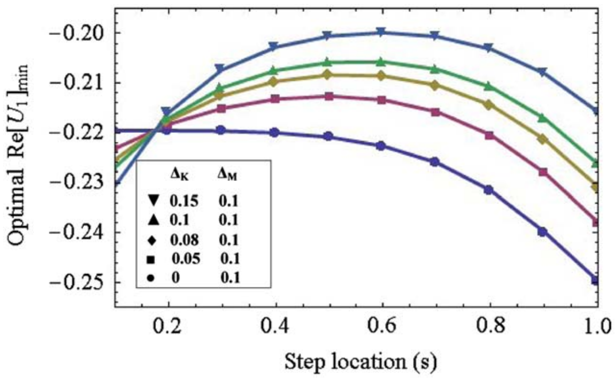

Fig. 10. Re$[U_1]_{\min}$ at optimal tuning of the DVA parameters and for step-like morphology of the beam.

Figs. 9 and 10 show the optimal chatter resistance as a function of s and variations in Δ_K and Δ_M, respectively. From Fig. 9 it is noted that: (a) for $\Delta_K=\Delta_M=0.1$ the optimal chatter resistance for $s=0.5$ is increased by 9 percent and 14.3 percent with respect to the homogeneous cases $s=1$ and $s=0$, respectively. (b) For $\Delta_K=0.1$ and $\Delta_M=0.05$ the optimal s is 0.6, which differs from the previous example ($s\cong 0.55$). (c) For $s\cong 0.85$ the optimal chatter resistance can be increased by Δ_K only and is independent of Δ_M. Fig. 10 reveals similar behavior with best resistance for the highest Δ_K at $s\cong 0.6$. A stiffness variation independent point is noted at $s\cong 0.18$.

An analytical approximation to the optimal step location s can be obtained by differentiating the FPM series by s and equalizing to zero. For simplicity we consider the first three FPM terms up to the first order in Δ_K and Δ_M:

$$\begin{pmatrix} (\sin(\psi)+\sinh(\psi))(\cos(s\psi)-\cosh(s\psi))+ \\ -(\cos(\psi)+\cosh(\psi))(\sin(s\psi)-\sinh(s\psi)) \end{pmatrix}^2 - \frac{\Delta_K}{\Delta_M}\begin{pmatrix} (\sin(\psi)+\sinh(\psi))(\cos(s\psi)+\cosh(s\psi))+ \\ -(\cos(\psi)+\cosh(\psi))(\sin(s\psi)+\sinh(s\psi)) \end{pmatrix}^2 = 0. \tag{55}$$

Note that (55) and therefore the optimal s are independent of the DVA parameters. For the private case $\Delta_K=\Delta_M$, one can obtain s explicitly:

$$s = \frac{1}{\psi}\arctan\left(\frac{\sin(\psi)+\sinh(\psi)}{\cos(\psi)+\cosh(\psi)}\right). \tag{56}$$

For a tuned DVA, the minimum of Re$[U_1]$ is located at $\psi=\psi^{(a)}$ or $\psi=\psi^{(n)}$; therefore the first chatter frequency will occur at $\psi=\psi^{(a)}$. For $\Delta_K=\Delta_M=0.1$ and for any s ($0<s<1$), $\psi^{(a)}$ is practically uniform ($1.77<\psi^{(a)}<1.79$). Inserting $\psi^{(a)}=1.77$ and 1.79 into (56) yields $s=0.529$ and 0.523 which are close to the optimal s obtained graphically (Fig. 9). Interestingly, this value is close to 0.5 which was originally used by Rivin and Kang [23].

6. Morphology optimization of mass and stiffness

In this chapter, the distributions of mass and stiffness along the bar are optimized for maximum chatter-resistance. This important subject had limited consideration (Rivin and Kang [23]), using lumped mass model, single step heterogeneity and simplified optimization criteria. Our aim is to obtain the optimal morphology restricted by a "physical" constraint which is also mathematically plausible.

We optimize the FPM solution (41) under the following constraints on morphology:

$$M'_{x_1} * M'_{x_1} = \mu^2; \quad K'_{x_1} * K'_{x_1} = \kappa^2. \tag{57}$$

μ and κ are "variation" measures for mass and stiffness, respectively.

Using the Lagrange multipliers' method we redefine the target function as follows:

$$\begin{aligned} R = {} & f^{(0)} + f^{(1)}_{x_1} * M'_{x_1} + f^{(2)}_{x_1} * K'_{x_1} + f^{(3)}_{x_1x_2} ** M'_{x_1} M'_{x_2} + f^{(4)}_{x_1x_2} ** K'_{x_1} K'_{x_2} + f^{(5)}_{x_1x_2} \\ & ** K'_{x_1} M'_{x_2} + \lambda_1 (M'_{x_1} * M'_{x_1} - \mu^2) + \lambda_2 (K'_{x_1} * K'_{x_1} - \kappa^2). \end{aligned} \tag{58}$$

where λ_1 and λ_2 are the Lagrange multipliers. Thus, by Lagrange method for variation problems the optimal morphology is obtained by

$$\frac{\partial R}{\partial \lambda_1} = 0; \quad \frac{\partial R}{\partial \lambda_2} = 0; \quad \frac{\delta R}{\delta M'_{x_3}} = 0; \quad \frac{\delta R}{\delta K'_{x_3}} = 0. \tag{59}$$

Thus we obtain the constraints on morphology (57), and coupled integral equations which are written here in a matrix format:

$$\mathbf{f}_{x_3} + \mathbf{g}_{x_1x_3} * \mathbf{P}'_{x_1} + 2\boldsymbol{\lambda}\mathbf{P}'_{x_3} = 0, \tag{60}$$

where,

$$\mathbf{P}'_{x_1} = \begin{bmatrix} M'_{x_1} \\ K'_{x_1} \end{bmatrix}; \quad \mathbf{f}_{x_3} = \begin{bmatrix} f^{(1)}_{x_3} \\ f^{(2)}_{x_3} \end{bmatrix}; \quad \boldsymbol{\lambda} = \begin{bmatrix} \lambda_1 & 0 \\ 0 & \lambda_2 \end{bmatrix}; \quad \mathbf{g}_{x_1x_3} = \begin{bmatrix} 2f^{(3)}_{x_1x_3} & f^{(5)}_{x_1x_3} \\ f^{(5)}_{x_3x_1} & 2f^{(4)}_{x_1x_3} \end{bmatrix}. \tag{61}$$

System (60) is a Fredholm integral equation of the second kind and its solution can be obtained by the Adomian's decomposition method [30]:

$$\mathbf{P}'_{x_3} = \sum_{i=1}^{\infty} \mathbf{P}'^{i}_{x_3}, \tag{62}$$

where,

$$\begin{aligned} \mathbf{P}'^{1}_{x_3} &= -\tfrac{1}{2}\boldsymbol{\lambda}^{-1}\mathbf{f}_{x_3} \\ \mathbf{P}'^{i+1}_{x_3} &= -\tfrac{1}{2}\boldsymbol{\lambda}^{-1}(\mathbf{g}_{x_1x_3} * \mathbf{P}'^{i}_{x_3}) \end{aligned} \tag{63}$$

However, it will be shown that the first-order approximation of the optimized morphology $\mathbf{P}'_{x_3} \cong \mathbf{P}'^{1}_{x_3}$ is sufficient for small μ and κ values and gives simple and explicit approximate solution. According to this approximation the Lagrange multipliers are (57):

$$\lambda_1 = \pm \frac{1}{2\mu}(f^{(1)}_{x_3} * f^{(1)}_{x_3})^{1/2}; \quad \lambda_2 = \pm \frac{1}{2\kappa}(f^{(2)}_{x_3} * f^{(2)}_{x_3})^{1/2}. \tag{64}$$

We choose appropriate signs for optimal response, i.e., negative for both λ_1 and λ_2. Therefore, the optimized morphologies are:

$$M'_{x_1} = \mu \frac{f^{(1)}_{x_1}}{(f^{(1)}_{x_3} * f^{(1)}_{x_3})^{1/2}}; \quad K'_{x_1} = \kappa \frac{f^{(2)}_{x_1}}{(f^{(2)}_{x_3} * f^{(2)}_{x_3})^{1/2}}. \tag{65}$$

Inserting (65) into (41) the approximated optimal response is:

$$R = f^{(0)} + \mu (f^{(1)}_{x_1} * f^{(1)}_{x_1})^{1/2} + \kappa (f^{(2)}_{x_1} * f^{(2)}_{x_1})^{1/2} + \mu^2 \frac{f^{(1)}_{x_1} * f^{(3)}_{x_1x_2} * f^{(1)}_{x_2}}{f^{(1)}_{x_3} * f^{(1)}_{x_3}} + \kappa^2 \frac{f^{(2)}_{x_1} * f^{(4)}_{x_1x_2} * f^{(2)}_{x_2}}{f^{(2)}_{x_3} * f^{(2)}_{x_3}} + \kappa\mu \frac{f^{(2)}_{x_1} * f^{(5)}_{x_1x_2} * f^{(1)}_{x_2}}{(f^{(2)}_{x_3} * f^{(2)}_{x_3})^{1/2} (f^{(1)}_{x_3} * f^{(1)}_{x_3})^{1/2}}. \tag{66}$$

System (60) can be also solved numerically by the quadrature (or Nystrom) methods [31]. Specifically, K_x' and M_x' are discretized into 10 increments and the quadrature rectangle rule is used on (60) to built a system of nonlinear algebraic equations with the unknowns of mass and stiffness vectors. Additional algebraic equations are given by the optimization method described in chapter 4, Eqs. (51)–(54), for determining the unknowns c and k. The optimized mass and stiffness are shown in Fig. 11 for three different μ and κ values (μ=κ). It can be seen that: (a) the analytical FPM approximation is very close to the numerical FPM solution; and (b) the optimized morphology form is kept as we increase both μ and κ.

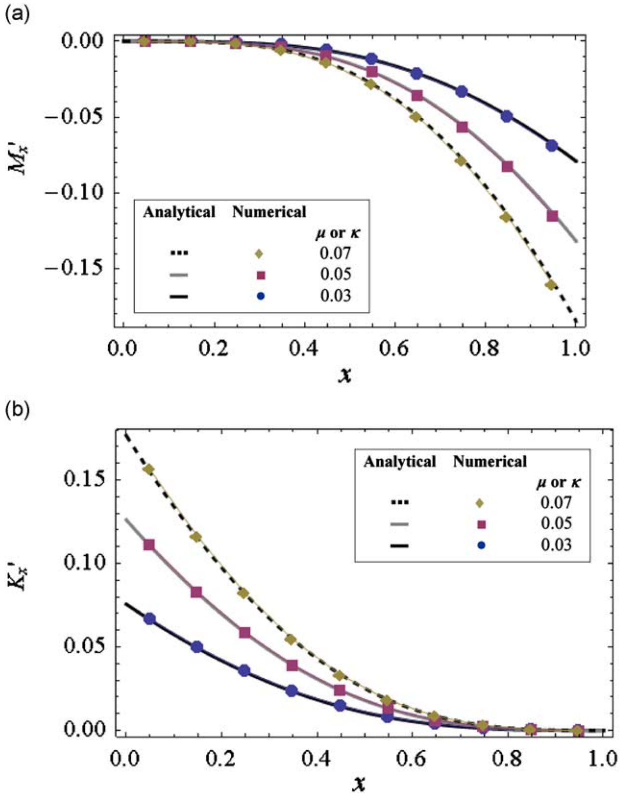

Fig. 11. Optimized morphology of: (a) M_x' and (b) K_x', for different κ and μ values ($\kappa=\mu$).

In general M_x' and K_x' are positively correlated and therefore it is fruitful to solve a correlated case, for example:

$$K_x' = \beta M_x' . \tag{67}$$

where β is constant. The target function is therefore:

$$R = f^{(0)} + F^{(1)}_{x_1} * M'_{x_1} + F^{(2)}_{x_1x_2} ** M'_{x_1} M'_{x_2} + \lambda(M'_{x_1} * M'_{x_1} - \mu^2). \tag{68}$$

where,

$$F^{(1)}_{x_1} + f^{(1)}_{x_1} + \beta f^{(2)}_{x_1}; \quad F^{(2)}_{x_1x_2} = f^{(3)}_{x_1x_2} + \beta^2 f^{(4)}_{x_1x_2} + \beta f^{(5)}_{x_1x_2}. \tag{69}$$

Then, by Lagrange method of variation we obtain:

$$F^{(1)}_{x_1} + (F^{(2)}_{x_1x_2} + F^{(2)}_{x_2x_1}) * M'_{x_2} + 2\lambda M'_{x_1} = 0; \quad M'_{x_1} * M'_{x_1} = \mu^2. \tag{70}$$

By Fredholm method, the solution of (70)-a is:

$$M'_{x_1} = \sum_{i=1}^{\infty} M'^{i}_{x_1}, \tag{71}$$

where,

$$M'^{1}_{x_1} = -\frac{1}{2\lambda} F^{(1)}_{x_1}$$

$$M'^{i+1}_{x_1} = -\frac{1}{2\lambda}(F^{(2)}_{x_1x_2} + F^{(2)}_{x_2x_1}) * M'^{i}_{x_2} \tag{72}$$

The first-order approximation of (72) ($M_x' \cong M'^{1}_x$) is considered and higher order terms are neglected, thus:

$$\lambda \cong -\frac{1}{2\mu}(F^{(1)}_{x_1} * F^{(1)}_{x_1})^{1/2}. \tag{73}$$

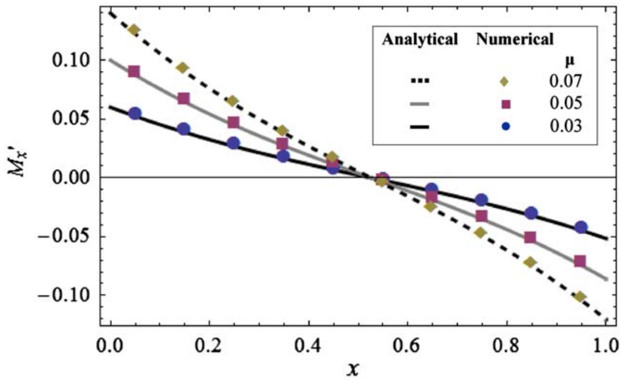

Fig. 12. Optimized M'_x for β=1 and different values of μ.

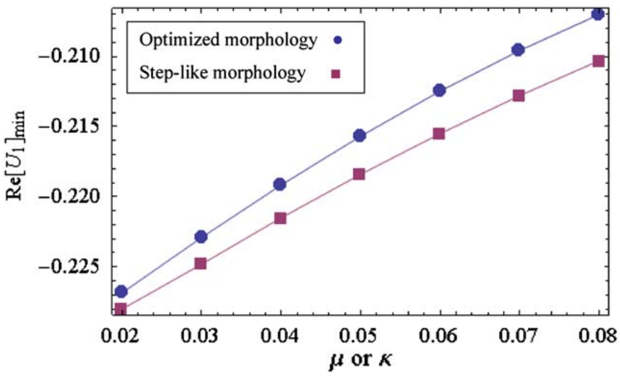

Fig. 13. Re[U_1] vs. μ or κ (μ=κ) for optimized and step-like morphologies (with optimized step location). For both morphologies the same constraint is determined and β=1.

The optimized morphology is therefore:

$$M'_{x_1} \cong M'^{1}_{x_1} = \mu \frac{F^{(1)}_{x_1}}{(F^{(1)}_{x_1} * F^{(1)}_{x_1})^{1/2}}. \tag{74}$$

And the response function is:

$$R = f^{(0)} + \mu(F^{(1)}_{x_1} * F^{(1)}_{x_1})^{1/2} + \mu^2 \frac{F^{(1)}_{x_1} * F^{(2)}_{x_1 x_2} * F^{(1)}_{x_2}}{F^{(1)}_{x_1} * F^{(1)}_{x_1}}. \tag{75}$$

Fig. 12 shows that the approximate analytical FPM solution is very close to the numerical one for small values of μ and κ. The optimal morphology distribution is practically linear and far from the "intuitive" single step solution of Rivin and Kang [23]. The zero deviation at $x \cong 0.5$ is also notable.

The optimal chatter resistance of the optimized morphology (obtained by the numerical quadrature method) is improved as we increase both μ and κ, and gives better resistance than the step-like morphology with optimized step-location, under the same constraints (57) (see Fig. 13).

7. Summary and conclusions

The FRF of a non-uniform cantilever beam with multiple spring-mass-dampers is obtained analytically by the FPM approximation up to the second order. The method is examined by comparing with the exact FRF of a step-like heterogeneous beam and single DVA. The results are found accurate for stiffness and mass variations, Δ_K and Δ_M, up to 20 percent.

The FPM solution is then used for optimizing the chatter-resistance of a heterogeneous tool holder with attached DVA. Sims approach for single dof system with DVA is generalized to the case of non-uniform (continuous) beams. The damping-invariant frequencies are obtained by a new method using the FRF of the damped system, avoiding singular response, rather than the undamped one.

Further increase in the chatter-resistance is achieved by searching for the best step location (s) for each Δ_K and Δ_M. For example, an improvement of 9 percent and 14.3 percent is achieved for $\Delta_K=\Delta_M=0.1$ with respect to the homogeneous cases $s=1$ and 0, respectively. Analytical approximation to the optimal s is obtained by the FPM, and found independent of the DVA parameters. It is also found that for some specific step locations the optimal response is independent of mass or stiffness variation.

Finally, the optimized morphology of a general heterogeneous beam with single DVA is derived by applying the Lagrange variation method on the FPM solution. It is found analytically that the optimized mass or stiffness deviation distribution is approximately proportional to the first functional derivative of the resistance function with respect to morphology. This yields a linear non-uniformity which is quite different from the well known Rivin and Kang [23] step-like design and improves the chatter-resistance.

Notations

$U_{x_1x_2\cdots x_n}$	a function U of n independent variables x_1, $x_2\ldots x_n$ (i.e. $U=U(x_1,x_2,\ldots,x_n)$)
$U_{x_1x_2\cdots x_n,x_ix_j\cdots x_k}$	partial derivatives of $U_{x_1x_2\ldots x_n}$ with respect to x_i, $x_j\ldots x_k$ (i, j, k=1,2,3,…)
$U_{x_1x_2} * V_{x_2}$	integral of $U_{x_1x_2}V_{x_2}$ over the region of x_2
$U_{x_1x_2x_3} * *V_{x_2}V_{x_3}$	double integral of $U_{x_1x_2x_3}V_{x_2}V_{x_3}$ over the rectangle defined by x_2 & x_3 regions
$J_{,K_{x_1}}$	1st functional derivative of a functional J by K_{x_1}, i.e. $J_{,K_{x_1}} = \delta J/\delta K_{x_1}$
$J_{,K_{x_1}M_{x_2}}$	2nd functional derivative of J by K_{x_1} and M_{x_2}, i.e. $J_{,K_{x_1}M_{x_2}} = \delta^2 J/(\delta K_{x_1}\delta M_{x_2})$
$\delta_{x_1x_2}$	Dirac's delta function: $\delta_{x_1x_2} \equiv \delta(x_1-x_2)$
M'_{x_1}	deviation of M_{x_1} from a reference one $M^{(0)}$, i.e. $M'_{x_1} = M_{x_1} - M^{(0)}$
Re(F)	real part of a complex function F
Abs(F)	magnitude of a complex function F

Acknowledgments

The authors gratefully acknowledge the partial support of ISCAR Company in Israel and the support of the Technion, Israel Institute of Technology.

References

[1] J.C. Snowdon, *Vibration and Shock in Damped Mechanical Systems*, Wiley, New York, 1968.
[2] L.A. Bergman, J.W. Nicholson, Forced vibration of a damped combined linear system, *Journal of Vibration, Acoustics, Stress, and Reliability in Design* 107 (1985) 275–281.
[3] J.W. Nicholson, L.A. Bergman, Free vibration of combined dynamical systems, *Journal of Engineering Mechanics* 112 (1986) 1–13.
[4] H.N. Ozguven, B. Candir, Suppressing the first and second responses of beams by dynamic vibration absorbers, *Journal of Sound and Vibration* 111 (1986) 377–390.
[5] D.N. Manikanahally, M.J. Crocker, Vibration absorbers for hysteretically damped mass–load beams, *ASME Journal of Vibration and Acoustics* 113 (1991) 116–122.
[6] M. Gúrgóze, Alternative formulations of the characteristic equation of a Bernoulli–Euler beam to which several viscously damped spring–mass systems are attached in span, *Journal of Sound and Vibration* 223 (1999) 666–677.
[7] J.S. Wu, D.W. Chen, H.M. Chou, On the eigenvalues of a uniform cantilever beam carrying any number of spring-damper-mass systems, *International Journal for Numerical Methods in Engineering* 45 (1999) 1277–1295.
[8] J.S. Wu, D.W. Chen, Dynamic analysis of a uniform cantilever beam carrying a number of elastically mounted point masses with dampers, *Journal of Sound and Vibration* 229 (3) (2000) 549–578.
[9] B.G. Korenev, L.M. Reznikov, *Dynamic Vibration Absorbers*, Wiley, England, 1993.
[10] J.J. Wu, Use of effective stiffness matrix for the free vibration analyses of a non-uniform cantilever beam carrying multiple two degree-of-freedom spring-damper-mass systems, *Computers and Structures* 81 (2003) 2319–2330.
[11] S. Nachum, E. Altus, Natural frequencies and mode shapes of deterministic and stochastic non-homogeneous rods and beams, *Journal of Sound and Vibration* 302 (4–5) (2007) 903–924.
[12] E. Altus, Microstress estimate of stochastically heterogeneous structures by the Functional Perturbation Method: a one dimensional example, *Probabilistic Engineering Mechanics* 21 (4) (2006) 434–441.
[13] J. Donies, L. Van Den Noortgate, Machining of Deep Holes without Chatter, *Note Technique* 10, Crif, Belgium 1974.
[14] L. Arnold, The mechanism of tool vibration in cutting of steel, *Proceedings of the Institution of Mechanical Engineers* 154 (1945) 261–276.
[15] J.P. Gurney, S.A. Tobias, A graphical analysis of regenerative machine tool instability, *Transaction ASME Journal of Engineering for Industry* 84 (1962) 103–112.
[16] J. Tlusty, A method of analysis of machine-tool stability, *International Journal of Machine Design and Research* 6 (1965) 5–14.
[17] N.H. Hanna, S.A. Tobias, The nonlinear dynamic behavior of a machine tool structure, *International Journal of Machine Tool Design and Research* 9 (3) (1969) 293–307.
[18] N. Deshpande, M.S. Fofana, Nonlinear regenerative chatter in turning, *Robotics and Computer Integrated Manufacturing* 17 (2001) 107–112.
[19] F.C. Moon, *Dynamics and Chaos in Manufacturing Processes*, Wiley, England, 1993.
[20] J. Tlusty, *Manufacturing Process and Equipment*, Prentice-Hall, NJ, 2000.
[21] H. Moradi, F. Bakhtiari-Nejad, M.R. Movahhedy, Tuneable vibration absorder design to suppress vibrations: an application in boring manufacturing process, *Journal of Sound and Vibration* 318 (2008) 93–108.
[22] J.P. Den Hartog, *Mechanical Vibrations*, fourth ed., McGraw-Hill, New York, 1956.
[23] E.I. Rivin, H. Kang, Enhancement of dynamic stability of cantilever tooling structures, *International Journal of Machine Tools and Manufacture* 32 (1992) 539–561.
[24] N.D. Sims, Vibration absorbers for chatter suppression: a new analytical tuning methodology, *Journal of Sound and Vibration* 301 (2007) 592–607.

[25] J.K. Liu, K.E. Rouch, Optimal passive vibration control of cutting process stability in milling, *Journal of Materials Processing Technology* 28 (1–2) (1991) 285–294.
[26] Y.S. Tarng, J.Y. Kao, E.C. Lee, Chatter suppression in turning operations with a tuned vibration absorber, *Journal of Materials Processing Technology* 105 (1) (2000) 55–60.
[27] J. Saffury, E. Altus, Optimized chatter resistance of viscoelastic turning bars, *Journal of Sound and Vibration* 324 (2009) 26–39.
[28] E.I. Rivin, Yu.E. Lapin, Cantilever tool Mandrel, US Patent No. 3,820,422 1974.
[29] J. Tlusty, M. Polacek, The stability of the machine tool against self excited vibration in machining, *Proceedings of the Production Engineering Research Conference on ASME*, Pittsburgh, 1963.
[30] A. Golbabai, B. Keramati, Easy computational approach to solution of system of linear Fredholm integral equations, *Chaos, Solitons and Fractals* 38 (2008) 568–574.
[31] K.E. Atkinson, *The Numerical Solution of Integral Equations of the Second Kind*, Cambridge University Press, Cambridge, 1997.
[32] M. Wiercigroch, A.M. Krivtsov, Frictional chatter in orthogonal metal cutting, *Philosophical Transactions of the Royal Society of London A* 359 (2001) 713–738.
[33] J. Warminski, G. Litak, M.P. Cartmell, R. Khanin, M. Wiercigroch, Approximate analytical solutions for primary chatter in the nonlinear metal cutting model, *Journal of Sound and Vibration* 259 (4) (2003) 917–933.
[34] E.P. Nosyreva, A. Molinari, Analysis of non-linear vibrations in metal cutting, *International Journal of Mechanical Sciences* 40 (1998) 735–748.
[35] G. Stépán, Delay-differential equation models for machine tool chatter, in: F.C. Moon (Ed.), *Dynamics and Chaos in Manufacturing Processes*, Wiley, 1998, pp. 165–191.